Robust Filter Design for a Re-Entry Vehicle

H. Castro[a], S. Bennani[a] and A. Marcos[b]
[a] Guidance Navigation and Control, ESA-ESTEC, The Netherlands
[b] Simulation & Control, Advanced Research Projects, Deimos Space S.L., Spain

Abstract

This paper describes the design of a robust $\mathcal{H}_\infty$ FDI filter for a re-entry vehicle with actuator faults. The filter is designed according to a model matching technique providing efficient isolation and actuator fault detection while rejecting external disturbances. Additive faults in the elevon and rudder actuators are considered. Robustness properties of the synthesized FDI system are obtained by design through explicit incorporation of uncertainty models reflecting desired design requirements. It is shown how to trade-off filter performance and robustness properties using frequency dependent weighting functions that reflect the shape of desired closed loop transfer functions. Validation of the inherited FDI filter properties is provided by means of time simulations.

Introduction

There has been a growing demand for reliability, maintainability, and survivability in dynamic systems. While in industrial processes the aim is for availability, i.e. to avoid inadvertent process shut-downs from simple failures, in the nuclear and aerospace industry, due to their high-risk applications, the aim is for fail-safe operation, i.e. no effects (or limited performance degradation) on system operation with single point failures. Such demand have led to increasing research in the area of reconfigurable/fault tolerant control systems.

Since the beginning it has been common practice to divide fault tolerance in functional independent levels such as fault detection & diagnosis, autonomous supervision and reconfiguration, [1]. As a result, on one hand most of the fault detection & diagnosis techniques are developed as a diagnostic or monitoring tool, rather than an integral part in the fault tolerant control system. On the other hand, most of the reconfigurable controls are carried out with the assumption of perfect information from fault detection and diagnosis, [2]. Although treated independently, they are still interconnected and must work together once in place. In this paper a fault detection and isolation (FDI) system is designed using the independent approach. However it is kept in mind that such system might be part of a reconfigurable system.

It is also general practice to design FDI filters in open-loop, although these are to work in a feedback, and hence closed-loop, system. The question whether the controller might interfere with the FDI filter performance arises. Isermann [4] states that the goal for the early detection and diagnosis is to have enough time for counteractions

such as reconfiguration, maintenance or repair. Furthermore he says that feedback systems hinder the early detection of process faults, and that advanced methods of supervision and fault diagnosis are needed. Moreover, Stoustrup and Niemann [3] concluded that for the nominal case there is a separation between the design of the feedback controller and the FDI filter which does not exist in the uncertain case. However, frequently in industry feedback controllers and FDI filters are designed by separated identities where information on requirements of each individual system is not always shared. In the end, once all the systems are assembled together they must achieve the required performance. This might complexify the verification and validation process.

The main objective in model-based FDI is the generation of residuals. A normal assumption in these model-based FDI techniques is that the mathematical model used is a faithful replica of the plant dynamics. Unfortunately in practice this never happens. Frequently the mathematical structure of the dynamic system or system parameters data are not fully known, or known only in a limited range. Thus, there is always a model-mismatch between the real plant dynamics and the model used for FDI design. This mismatch in modeling the plant dynamics and faults can either cause a high false alarm rate, or make it difficult to detect failures, [12]. Therefore, the challenge in FDI filters design, in presence of disturbances, uncertainties and noise, is the generation of a residual which is insensitive to these disturbances, uncertainties and noise and sensitive to fault signals, [17, 5]. This is so, because uncertainties and faults both act upon the diagnostic signal (residual). Therefore, there must be a discrimination between fault-induced changes and variations due to uncertainty. Usually this leads to a trade-off between sensitivity and robustness. Nevertheless, even in the ideal case of no disturbances, sensitivity to faults is still required for residuals.

Qiu *et al.* [9] say that many FDI methods were provided with some way of eliminating or minimizing the effect of disturbances and modeling errors. Many of these methods were developed for ideal systems or special noises and then efforts have been made to include non-ideal or more general uncertainties, [6]. While this is possible for structured disturbances or modeling errors, the same can not be said for unstructured disturbances/modeling errors. In contrast, $\mathcal{H}_\infty$-optimization is a robust multivariable design method with the original motivation firmly rooted in the consideration of various uncertainties including unstructured. $\mathcal{H}_\infty$-optimization methods were first proposed for FDI design in Viswanadham and Minto, [7]. In references [7] to [17] several FDI filter solutions are given using $\mathcal{H}_\infty$ based methods. Earlier solutions were based in coprime factorization, [7, 8, 9, 10, 14]. In later references [15, 16, 17] $\mathcal{H}_\infty$ filters are solutions of the Algebraic Riccati equation with different optimization indexes. Also recently, solutions appeared in terms of linear matrix inequalities (LMIs), [11, 21]. Applications of $\mathcal{H}_\infty$-based FDI filters are presented in Stoustrup and Niemann [18] for the three tank system, in Marcos *et al.* [19] for a Boeing 747 aircraft, in Marcos *et al.* [20] for a turbofan engine and in Grenaille *et al.* [21] for a satellite.

The paper is organized as follows. First we shall review the analysis results coming from the general $\mathcal{H}_\infty$ fault diagnosis theory [3, 17, 20] in order to set the termi-

nology used in this paper. Having mathematically formalized the $\mathcal{H}_\infty$ FDI problem formulation we briefly present the re-entry vehicle system dynamics [24] including a description of the fault scenario, controller and other components needed for the development and analysis of the FDI filter. Then we present the actual filter design consisting of an appropriate filter architecture formulated as a weighted model matching interconnection structure [17, 19]. The choice of the functional constraints to be optimized is expressed in terms of transfer function shaping [3, 20]. The performance and robustness properties of the designed filter are validated using linear simulations.

Problem formulation & Analysis

The general filtering problem can be translated as: estimate the unknown faults in a system given all known inputs and outputs of the plant G. In the $\mathcal{H}_\infty$ filter design problem usually some index is minimized when designing the filter. In the present case a method similar to the model-matching tracking problem is to be used. Therefore, the index to be minimized is the weighted error between an ideal fault model and the generated residual, $e = W_e\left(W_f f - \hat{f}\right)$. This formulation is better seen in figure 1. In this figure d represents all disturbances and f all faults that act over the system. The vector $(y\ u)^T$ is the system outputs and inputs which are fed to the filter block to generate the fault estimation $\hat{f}$. Filter weighting functions W_e and W_f are used in order to emphasize the desired frequency range for the fault estimation.

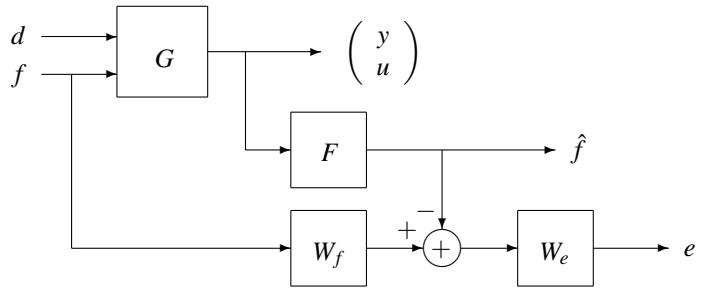

Figure 1: $\mathcal{H}_\infty$ filter design problem

The robust $\mathcal{H}_\infty$ filter design problem is then described as: given all known system inputs and outputs, design a filter capable to estimate the faults present in the system for a given uncertainty set. Thus, the fault estimation error, e, is minimized for the given uncertainty set. A linear fractional representation of the general robust filter design problem is presented in figure 2. In this figure f represents all faults entering the system; d represents disturbances such as pilot inputs, u, sensor noise, n, and gusts, g; u_F and y_F are the filter input and output, while z and w are the uncertainty input and output respectively; e is the fault estimation error.

From figure 2, the nominal $\mathcal{H}_\infty$ filter design problem results in designing a stable

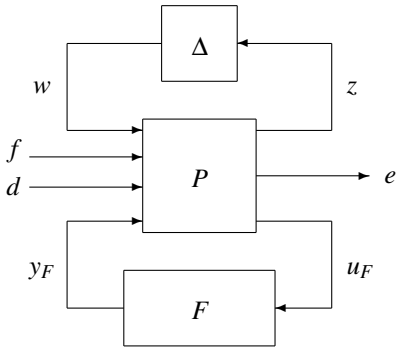

Figure 2: General filter problem

filter F such that the fault estimation error is minimized assuming $\Delta = 0$. This is equivalent to inequality 1, where $F_l(P,F)$ denotes the lower linear transformation of P and F, and γ is a positive constant that defines the nominal performance level (i.e. the nominal FDI filter performance). The robust $\mathcal{H}_\infty$ filter design problem is to find a stable filter F such that the fault estimation error is minimized for all values of the uncertainty set. This is equivalent to inequality 2. In the same way, γ_R gives the robust performance level, and one can talk in terms of robust filter performance.

$$||F_l(P,F)||_\infty < \gamma \tag{1}$$

$$||F_u(\Delta,M)||_\infty = ||F_u(\Delta,F_l(P,F))|| < \gamma_R \tag{2}$$

The goal of this paper is to design a robust FDI filter which detects and isolates actuator faults in the presence of external disturbances and uncertainties. In figure 3 an interconnection structure for the fault estimation problem is shown. System G represents a re-entry vehicle in landing phase with two control surfaces: elevon and rudder. System G_{act} is a diagonal transfer matrix which contains the elevon and rudder actuator transfer functions. Moreover, each actuator output is affected by additive faults as shown. The interconnection disturbances are pilot commands, gusts, and sensor noise, $d = \begin{pmatrix} u & g & n \end{pmatrix}^T$. Multiplicative uncertainty at the actuators input, Δ_a, is considered, as well as parametric model uncertainty, Δ_p, due to the aerodynamic data variation at the flight condition considered. Using a partition of G as given in equation 3, interconnection P is calculated from figure 3 as shown in equations 4 and 5.

$$\begin{pmatrix} z \\ y \end{pmatrix} = \begin{pmatrix} G_{zw} & G_{z\theta} & G_{zd_g} \\ G_{yw} & G_{y\theta} & G_{yd_g} \end{pmatrix} \begin{pmatrix} w \\ \theta \\ d_g \end{pmatrix} \tag{3}$$

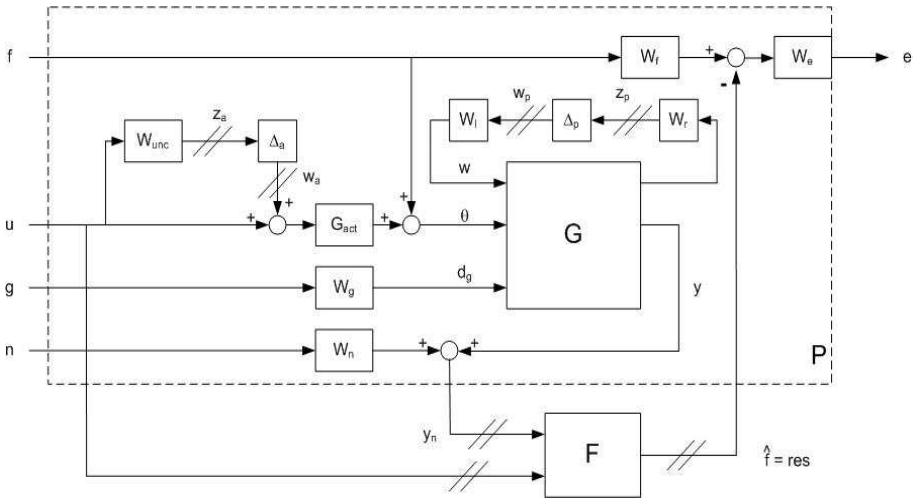

Figure 3: Filter design interconnection

$$\begin{bmatrix} z_p \\ \hline z_a \\ \hline e \\ \hline y_n \\ u \end{bmatrix} = P \begin{bmatrix} w_p \\ \hline w_a \\ \hline f \\ u \\ g \\ n \\ \hline res \end{bmatrix} = \left[\begin{array}{c|c|c} P_{11} & P_{12} & P_{13} \\ \hline P_{21} & P_{22} & P_{23} \\ \hline P_{31} & P_{32} & P_{33} \end{array}\right] \begin{bmatrix} w_p \\ \hline w_a \\ \hline f \\ u \\ g \\ n \\ \hline res \end{bmatrix} \tag{4}$$

$$P = \left[\begin{array}{cc|c|cccc} W_r G_{zw} W_l & W_r G_{z\theta} G_{act} & W_r G_{z\theta} & W_r G_{z\theta} G_{act} & W_r G_{z d_g} W_g & 0 & 0 \\ 0 & 0 & 0 & W_{unc} & 0 & 0 & 0 \\ \hline 0 & 0 & W_e W_f & 0 & 0 & 0 & -W_e \\ \hline G_{yw} W_l & G_{y\theta} G_{act} & G_{y\theta} & G_{y\theta} G_{act} & G_{y d_g} W_g & W_n & 0 \\ 0 & 0 & 0 & I & 0 & 0 & 0 \end{array}\right] \tag{5}$$

$$\begin{bmatrix} z_p \\ \hline z_a \\ \hline e \end{bmatrix} = M \begin{bmatrix} w_p \\ \hline w_a \\ \hline f \\ u \\ g \\ n \end{bmatrix} = \left[\begin{array}{c|c} M_{11} & M_{12} \\ \hline M_{21} & M_{22} \end{array}\right] \begin{bmatrix} w_p \\ \hline w_a \\ \hline f \\ u \\ g \\ n \end{bmatrix} \tag{6}$$

The lower linear fractional transformation $F_l(P,F)$ is given in equation 6, where each partition is calculated using equation 7. Furthermore, since $P_{13}(s) = P_{21}(s) =$

$P_{33}(s) = 0$, equations 8 to 11 result. Finally, giving a filter F partitioned as in equation 12, the M matrix of equation 6 is as shown in equation 13.

$$\begin{aligned} M_{ij}(s) &= P_{ij}(s) + P_{i3}(s)\left[I(s) - F(s)P_{33}(s)\right]^{-1} F(s)P_{3j}(s) \\ i,j &= 1,2 \end{aligned} \tag{7}$$

$$M_{11}(s) = P_{11}(s) \tag{8}$$
$$M_{12}(s) = P_{12}(s) \tag{9}$$
$$M_{21}(s) = P_{23}(s)F(s)P_{31}(s) \tag{10}$$
$$M_{22}(s) = P_{22}(s) + P_{23}(s)F(s)P_{32}(s) \tag{11}$$

$$res = \begin{pmatrix} r_{ele} \\ r_{rud} \end{pmatrix} = \begin{pmatrix} F_y & F_u \end{pmatrix} \begin{pmatrix} y_n \\ u \end{pmatrix} \tag{12}$$

$$M = \left[\begin{array}{cc|cc} W_r G_{zw} W_l & W_r G_{z\theta} G_{act} & W_r G_{z\theta} & W_r G_{z\theta} G_{act} \\ 0 & 0 & 0 & W_{unc} \\ \hline -W_e F_y G_{yw} W_l & -W_e F_y G_{y\theta} G_{act} & W_e\left(W_f - F_y G_{y\theta}\right) & -W_e\left(F_y G_{y\theta} G_{act} + F_u\right) \end{array}\right.$$
$$\left.\begin{array}{cc} W_r G_{zd_g} W_g & 0 \\ 0 & 0 \\ \hline -W_e F_y G_{yd_g} W_g & -W_e F_y W_n \end{array}\right] \tag{13}$$

As mentioned before, the FDI filter in the nominal case should minimize the fault estimation error, as given by equation 1. This is equivalent to $||M_{22}||_\infty < \gamma$. Thus, using equation 13 it is possible to analyze the contribution of faults, f, and disturbances, d, to the fault estimation error. Inequality 14 gives the possibility to maximize the faults and to minimize the disturbance effects in the fault estimation, by carefully choosing the adequate values for the weighting functions. In other words, since we use a model-matching problem, F_y and F_u should approximate a described behavior imposed by W_f and W_e related to the conditions derived from inequality 14. From Small Gain theorem [22, 23], conditions 15 to 18 follow.

$$\left\| \begin{pmatrix} W_e\left(W_f - F_y G_{y\theta}\right) \\ -W_e\left(F_y G_{y\theta} G_{act} + F_u\right) \\ -W_e F_y G_{yd_g} W_g \\ -W_e F_y W_n \end{pmatrix}^T \right\|_\infty < \gamma \tag{14}$$

$$||W_e\left(W_f - F_y G_{y\theta}\right)||_\infty < \gamma_1 \quad \Leftrightarrow \quad ||F_y G_{y\theta}||_\infty < \left|\left|\frac{\gamma_1}{W_e}\right|\right|_\infty + \left|\left|W_f\right|\right|_\infty \tag{15}$$

$$||-W_e\left(F_y G_{y\theta} G_{act} + F_u\right)||_\infty < \gamma_2 \quad \Leftrightarrow \quad ||F_u||_\infty < \left|\left|\frac{\gamma_2}{W_e}\right|\right|_\infty + ||F_y G_{y\theta} G_{act}||_\infty \tag{16}$$

$$||-W_e F_y G_{yd_g} W_g||_\infty < \gamma_3 \quad \Leftrightarrow \quad ||F_y G_{yd_g}||_\infty < \left|\left|\frac{\gamma_3}{W_e W_g}\right|\right|_\infty \tag{17}$$

$$||-W_e F_y W_n||_\infty < \gamma_4 \quad \Leftrightarrow \quad ||F_y||_\infty < \left|\left|\frac{\gamma_4}{W_e W_n}\right|\right|_\infty \tag{18}$$

Inequalities 15 and 17 impose conditions to the norm of $F_y G_{y\theta}$ and $F_y G_{yd_g}$ respectively. On the other hand inequality 18 imposes a condition directly to the norm of F_y. Lastly, inequality 16 imposes a condition to the norm of F_u. Once a desired nominal filter performance level, $\gamma = max(\gamma_1, \gamma_2, \gamma_3, \gamma_4)$, is achieved, the filter design can be further optimized until a robust filter performance level, γ_R is achieved, as stated in inequality 2. This results in inequality 19. Now, since the uncertainty considered (multiplicative Δ_a and parametric Δ_p) is structured, the filter design can be calculated using the structured singular value, μ, where it is imposed $\mu_\Delta(M_\Delta) < \gamma_R$. Furthermore, in the particular case of considering only multiplicative uncertainty, $M_{11} = 0$ and inequality 19 becomes inequality 20. In other words, the robust filter performance will be equal to the nominal filter performance plus the cross-coupling effects.

$$||F_u(\Delta, M)||_\infty < \gamma_2 = ||M_{22} + M_{21}\Delta\left(I - M_{11}\Delta\right)^{-1} M_{12}||_\infty < \gamma_R \tag{19}$$

$$||M_{22} + M_{21}\Delta M_{12}||_\infty < \gamma_R \tag{20}$$

System dynamics

The re-entry vehicle model is taken from [24]. This is a simplified lateral-directional model of the Space Shuttle, in the final stages of landing as it transitions from supersonic to subsonic speeds. It is a rigid body model at Mach 0.9 with four-state variables: sideslip angle, roll rate, yaw rate and bank angle, $x = \begin{bmatrix} \beta & p & r & \phi \end{bmatrix}^T$. An input/output block diagram of the aircraft is shown in figure 4. The first input is the actual angular deflection of the elevon surface. The second is the actual deflection of the rudder surface. The last input is a lateral wind gust disturbance, due to the winds that occur at this altitude. The aircraft has two controlled inputs: rudder and elevon commands. Each actuator is modeled with a second order transfer function, as well as a second order delay approximation to model the effects of digital implementation. See the details of the LTI plant and actuators in [24].

The major source of uncertainty in the aircraft model is in the aerodynamic coefficients. At this flight condition (i.e. transonic regime), theoretical, computational, and

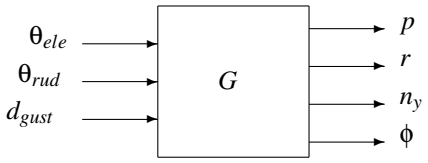

Figure 4: Aircraft block diagram

wind tunnel techniques are inaccurate. Uncertainty in the aerodynamic coefficients is modeled as a nominal value plus a perturbation, e.g. $c_{y_\beta} = \bar{c}_{y_\beta} + r_{y_\beta}\delta_{y_\beta}$. The perturbations δ_{ij} are assumed to be fixed, unknown, real parameters, each satisfying $|\delta_{ij}| < 1$. For more information over the values of $\bar{c}_{ij}$ and r_{ij} referred to [24]. All variables in the output are measured with inertial devices whose individual noise characteristics becomes more severe with increasing frequency. The frequency response of the p, r, ϕ and n_y noise weighting functions can be seen in figure 5. A gust weighting function representing typical wind gusts, encountered at this flight condition is also given in [24], see figure 5. As mentioned before, although the FDI filter is designed in open-loop, it is supposed to perform in closed-loop. Therefore during the time simulations three different controllers, k_h, k_x and k_{mu} taken from [24] will be used for analysis. k_h was designed to optimize nominal $\mathcal{H}_\infty$ performance; k_{mu} was optimized for robust performance using μ-synthesis; k_x was designed to be a trade-off between the two previous controllers. All controllers were optimized for good tracking of pilot bank-angle command, turn coordination and minimization of lateral acceleration. A worst case performance analysis was done in [24] and it was concluded that controller k_{mu} presented the best performance to increasing uncertainty, i.e. more robustness. Controller k_h had the best nominal performance but degraded too rapidly for small amounts of uncertainty, i.e. no robustness.

Filter design

The filter was designed based on the interconnection presented in figure 3, considering only the multiplicative uncertainty at actuators input, Δ_a. The parametric uncertainty, Δ_p was used only during time simulations. Since elevon and rudder controls are considered, signals u, f, res and e in figure 3 are signal vectors of two components each, and G_{act}, W_{unc}, W_f and W_e are two by two diagonal weighting matrices. The robust $\mathcal{H}_\infty$ FDI filter design is an iterative process where some weighting functions are "tuning parameters" used to achieve a certain desirable performance level. In the previous section, noise and gust weighting functions were chosen according to what is known from the system at the selected flight condition. Thus, these were kept fixed during the design process. The fault model (W_f), the fault estimation error (W_e) and the uncertainty (W_{unc}) weighting functions were defined during the design, and hence used to tune the filter design. The initial values used for these weighting functions

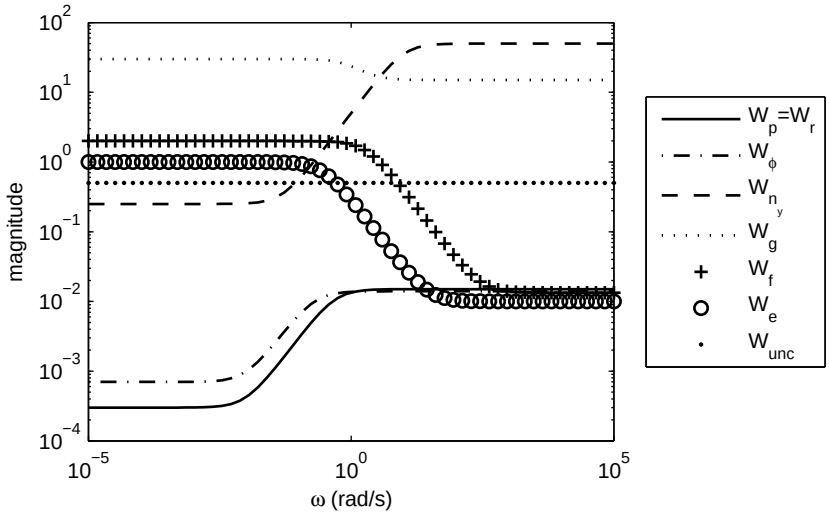

Figure 5: Frequency response of sensor noise and gust weighting functions

were taken as given in [19], see equations 21 to 23 and figure 5. The weighting functions are presented in the form $W(s) = \frac{s/H+\omega_B}{s+\omega_B A}$, since in this way it is directly seen what the weighting function bandwidth is, as well as the value at frequency $s = 0$, $W(s=0) = \frac{1}{A}$, and at $s = \infty$, $W(s=\infty) = \frac{1}{H}$. Using the previous weighting functions and taking into account that only multiplicative uncertainty is used, a filter was designed so that inequality 17 was fulfilled.

$$W_f(s) = \frac{s/75+4}{s+4*0.5} \quad (21)$$

$$W_e(s) = \frac{s/100+0.3}{s+0.3} \quad (22)$$

$$W_{unc}(s) = 0.5 \quad (23)$$

A γ value of 1.4142 was achieved in this first design as shown in figure 6. Since γ is bigger than 1, it is concluded that the design objectives are not fulfilled. It is also shown in figure 6 that $M_{22} = M_{21}$, each contributing with a value of about 1 for the total M_Δ at low frequencies. From inequality 20 it is seen that the cross-coupling effects, contribution from $M_{21}\Delta M_{12}$, adds up to the contribution from nominal performance, M_{22}. Since $||M_{22}||_\infty = 1$, the robust performance level can become only higher than 1, $||M_\Delta||_\infty > 1$. Therefore, in order to improve robust performance, nominal performance has to be improve to a level $\gamma < 1$. In order to find which conditions are pushing M_{22} at low frequencies, in figure 7 the right-hand terms of inequalities 15 to 18 are plotted against the left-hand terms, supposing performance levels $\gamma_i = 1$.

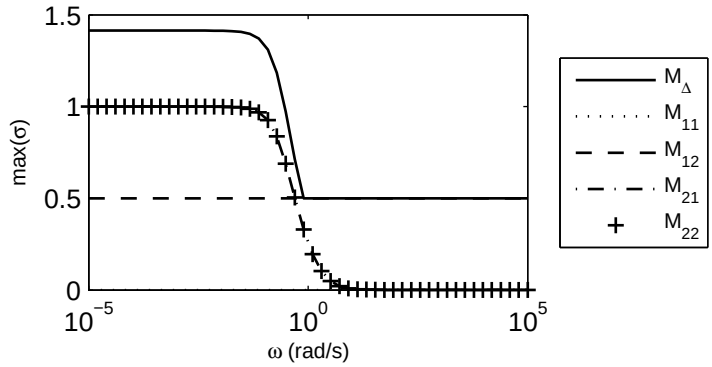

Figure 6: Maximum singular values

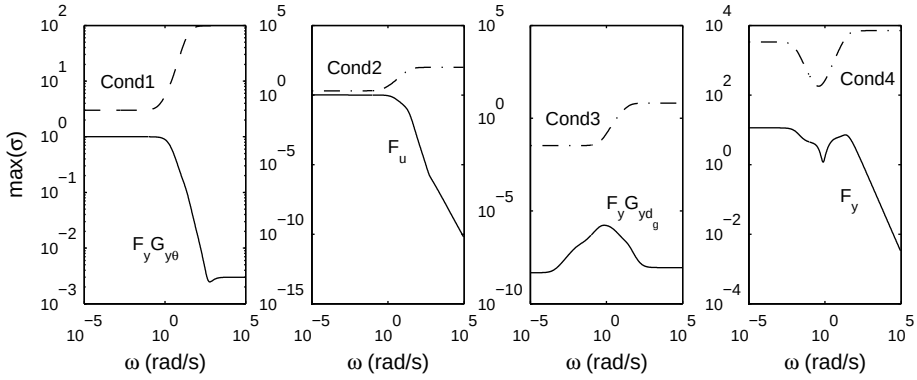

Figure 7: Singular value analysis

In figure 7 it is seen that *Cond*2, i.e. inequality 16, is just fulfilled. A look at inequality 16 reveals that W_e is the only weighting function which can still be changed. The easiest way is to scale down W_e by 1.42 making the requirement in the fault estimation error less stringent as shown in equation 24. To scale down W_e by 1.42 is equivalent to decrease the bandwidth, increase the transient dynamics (given by H) and increase the allowed steady state error (given by A). With this new error weighting function a new filter was designed which achieved a γ of 0.996. The filter frequency response is presented in figures 8 and 9. In figure 8 it is seen that residual r_{rud} is more influenced by the system outputs p, r, n_y and ϕ than residual r_{ele}. Besides, the yaw rate r has the biggest influence, while the influence of lateral acceleration, n_y, is the smallest. On figure 9 it is well seen the decoupling between residuals. While, at low frequencies, r_{ele} is influenced by input u_{ele}, residual r_{rud} is influenced by input u_{rud}.

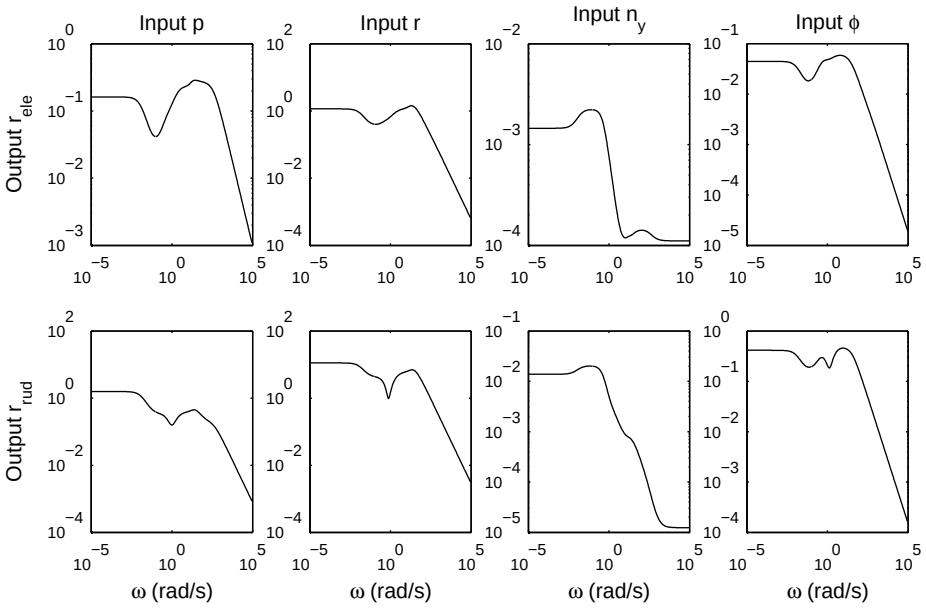

Figure 8: Filter frequency response (F_y)

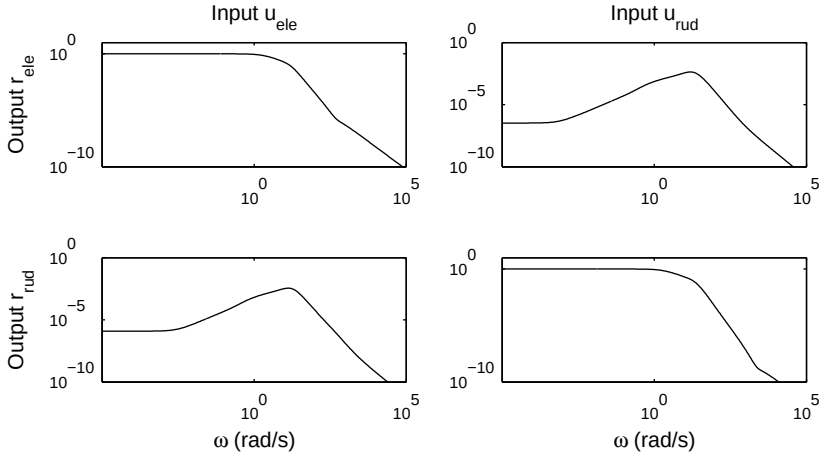

Figure 9: Filter frequency response (F_u)

$$W_e(s) = \frac{1}{1.42}\frac{s/100+0.3}{s+0.3} = \frac{s/142+0.21}{s+0.21*1.42} \tag{24}$$

The fault estimation for the nominal case using this filter is presented in figure 10 for the open-loop case and for the closed-loop case using the three previous controllers (k_h, k_x and k_{mu}). It is seen that the filter has the same performance for the open-loop and the closed-loop system since the time response for the four different cases are the same. This is as expected since no uncertainty is considered. Furthermore, good estimation is achieved since the fault estimation follows the introduced faults within a detection time of about 2.5 seconds. It is also observed that the residuals are practically decoupled for both the elevator and rudder actuator faults, as previewed in figure 9.

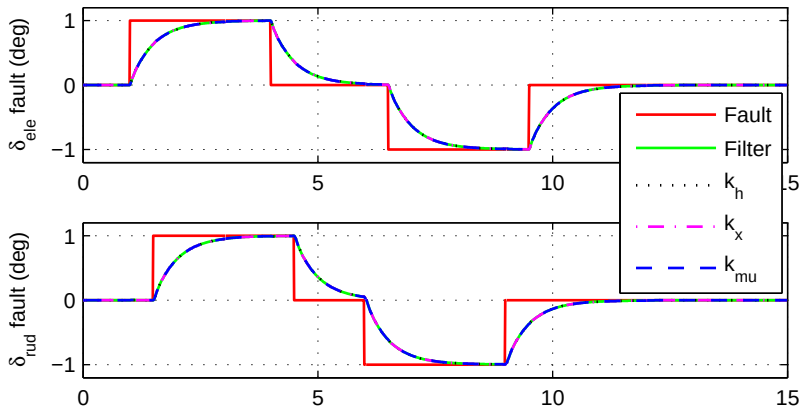

Figure 10: Nominal fault estimation time response

To improve the detection time the different parameters of the fault and fault estimation error weighting functions were changed. The fault estimation error weighting, W_e, is the responsible for the filter performance. However, it was found that changing this weighting function bandwidth and H parameter did not influence the filter design, and thus the fault detection. As it would be expected, the A value from W_e is related to the steady state error, and influences directly the value of γ. Thus, decreasing A in an amount of 10 or 100 times, increases the γ value in the same amount, showing that it is the steady state error which drives the filter design at low frequencies. However, none of these parameters improved the fault detection time. Therefore, attention turned to the fault estimation weight, W_f.

In a similar way as for the tracking case in a controller design, the fault model weighting, W_f, is supposed to represent the model of the fault to be estimated. A first order transfer function, a high pass filter in this case, is used to identify step-like faults. It was found that by changing the bandwidth, ω_B, of this weight the filter would detect faults faster. Furthermore, increasing parameter H influences the transient dynamics of the detection, thus this was not changed. Increasing or decreasing the value of A would affect the magnitude of the fault estimation and the value of γ. A value of $A = 0.5$ was found to be good in order to follow the faults correctly. Thus, the fault model weight was changed to that of equation 25 where it is seen the bandwidth has

increased from a value of $\omega_B = 4rad/sec$ to $\omega_B = 20rad/sec$. A filter was designed which still achieved the same value of $\gamma = 0.996$ and has faster detection time as shown in figure 11.

$$W_f(s) = \frac{s/75 + 20}{s + 20 * 0.5} \tag{25}$$

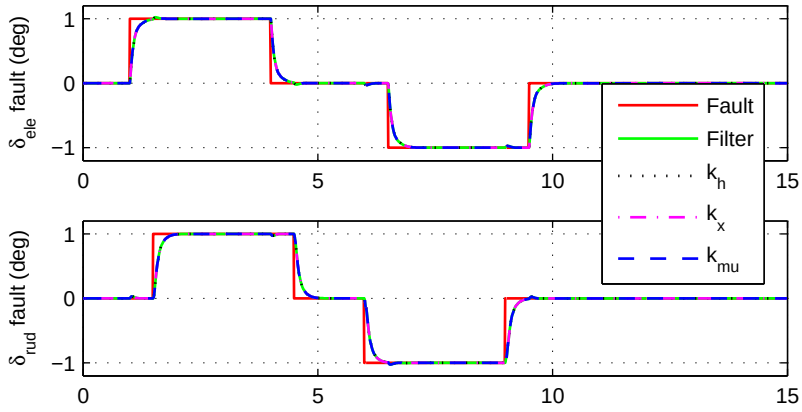

Figure 11: Nominal fault estimation time response with faster filter

The uncertainty weighting function, W_{unc}, establishes how much uncertainty is allowed in the actuator and system dynamics keeping the performance level acceptable. A constant of 0.5 is used which means that relative uncertainty of 50% is allowed. For changes in this constant from 0.5 up to 0.996 the value of γ does not change. This means that up to a level of 0.996 the uncertainty does not drive the γ minimization, as concluded above. However, if the magnitude of W_{unc} increases above 0.996 the value of γ will increase as well, i.e. the filter design will be driven by the uncertainty weighting function. On the other hand, in figure 6 it is seen that at high frequencies M_Δ, as well as M_{22} and M_{21}, have low values (roll-off). Therefore, from equations 20 and 9 the tolerance to uncertainty can be increased until 100% relative uncertainty at high frequencies while keeping the same 50% relative uncertainty at low frequencies, see equation 26. It is very usual to use high pass filters for input multiplicative uncertainty in aircraft control design when neglecting phugoid and spiral dynamics. A new filter design was done achieving a γ value of exactly 1 at almost all frequencies.

$$W_{unc}(s) = \frac{s + 0.4}{s + 0.4 * 2} \tag{26}$$

In figure 12, the fault detection is shown when the plant is disturbed with 40% of the k_{mu} worst case parametric uncertainty given in [24]. In order to better see the

fault detection robustness to parametric uncertainty, no bank angle is commanded. It is seen in figure 12 that filter estimation is better achieved for the closed-loop cases with the robust controllers, k_x and k_{mu}.

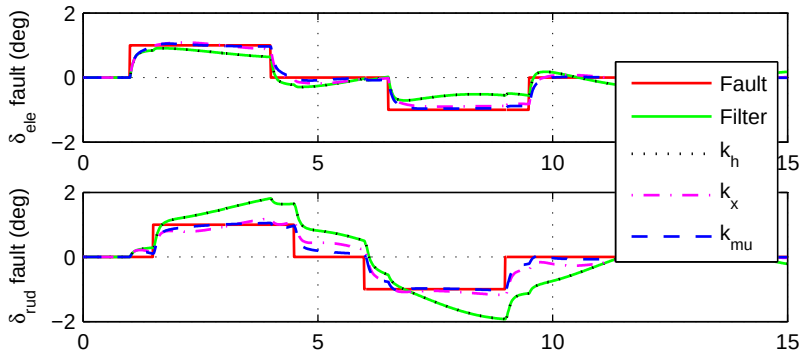

Figure 12: Fault estimation response with 40% parametric uncertainty

CONCLUSIONS

An H_∞ filter was designed to detect additive faults in two different actuators: elevon and rudder. Linear time simulations were carried out using three different controllers: one with no robustness characteristics and two other robust. After tuning the weighting functions of the FDI filter, a fast and accurate detection and isolation was achieved for the nominal case (i.e. no system uncertainty). For the perturbed case, good fault estimation is achieved only in the case of closed-loops formed with the robust controllers, hence suggesting that a robust controller is useful to compensate for the uncertainty effects during fault detection. Furthermore, in case some kind of control reconfiguration is not present, robustness to faults is also necessary, otherwise the system is lost and fault detection is no more possible.

References

[1] M. Blanke, M. Staroswiecki and N. E. Wu, "Concepts and methods in fault tolerant control", in *Proceedings of the American Control Conference*, June 2001.

[2] Y. Zhang and J. Jiang, "Bibliographical review on reconfigurable fault-tolerant control systems", in *Proceedings of the IFAC Symposium on Fault Detection, Supervision and Safety for Technical Processes*, Washington DC, USA, pp. 257-268, 2003.

[3] J. Stoustrup, M. J. Grimble and H. Niemann, "Design of integrated systems for the control and detection of actuator/Sensor faults", in *Sensor Review*, Vol. 17, No. 2, pp. 138-149, July 1997.

[4] R. Isermann, "Supervision, fault-detection and fault-diagnosis methods - An Introduction", in *Control Engineering Practice*, Vol. 5, No. 5, pp. 639-652, 1997.

[5] H. H. Niemann, A. Saberi, A. A. Stoorvogel and P. Sannuti, "Optimal fault estimation", in *IFAC SAFEPROCESS'2000*, Budapest, Hungary, pp. 262-267, June 2000.

[6] R. J. Patton and J. Chen, "Observer-based fault detection and isolation: Robustness and applications", in *Control Engineering Practice*, Vol. 5, No. 5, pp. 671-682, 1997.

[7] N. Viswanadham and K. D. Minto, "Robust observer design with application to fault detection", in *Proceedings of the American Control Conference*, Atlanta, GA, pp. 1393-1399, June 1988.

[8] X. Ding and P. M. Frank, "Fault detection via factorization approach", in *Systems and Control Letters*, Vol. 14, pp. 431-436, 1990.

[9] Z. Qiu and J. Gertler, "Robust FDI Systems and $\mathcal{H}_\infty$ optimization: Disturbances and tall fault case", in *IEEE Proceeding of the conference on Decision and Control*, San Antonio, TX, USA, pp. 1710-1715, December 1993.

[10] P. M. Frank and X. Ding, "Frequency domain approach to optimally robust residual generation and evaluation for model-based fault diagnosis", in *Automatica*, Vol. 30, No. 5, pp. 789-804, 1994.

[11] A. Edelmayer, J. Bokor and L. Keviczky, "An $\mathcal{H}_\infty$ filtering approach to robust detection of failures in dynamical systems", in *Proceedings of the 33rd IEEE Conference on Decision and Control*, Vol. 3, pp. 3037-3039, 1994.

[12] R. S. Mangoubi, B. D. Appleby, G. C. Verghese and W. E. van der Velde, "A robust failure detection and isolation algorithm", in *Proceedings of the 34rd IEEE Conference on Decision and Con trol*, Vol. 3, pp. 2377-2382, 1995.

[13] P. M. Frank and X. Ding, "Survey of robust residual generation and evaluation methods in observer-based fault detection systems", in *Journal of Proccess Control*, Vol. 7, No. 6, pp. 403-424, 1997.

[14] X. Ding and L. Guo, "On observer based fault detection", in *Proceedings of the IFAC Symposium on Fault Detection, Supervision and Safety for Technical Processes*, Kingston Upon Hull, UK, pp. 115-123, 1997.

[15] D. Sauter, F. Rambeaux and F. Hamelin, "Robust fault diagnosis in an $\mathcal{H}_\infty$ setting", in *Proceedings of the IFAC Symposium on Fault Detection, Supervision and Safety for Technical Processes*, Kingston Upon Hull, UK, pp. 869-874, 1997.

[16] M. A. Sadrnia, J. Chen and R. J. Patton, "Robust $\mathcal{H}_\infty/\mu$ observer-based residual generation for fault diagnosis", in *Proceedings of the IFAC Symposium on Fault Detection, Supervision and Safety for Technical Processes*, Kingston Upon Hull, UK, pp. 155-161, 1997.

[17] J. Chen and R. J. Patton, "$\mathcal{H}_\infty$ formulation and solution for robust fault diagnosis", in *14th Triennial World Congress of IFAC*, Beijing, P. R. Chine, pp. 127-132, 1999.

[18] J. Stoustrup and H. Niemann, "Application of an $\mathcal{H}_\infty$ based FDI and control scheme for the three tank system", in *Proceedings of the IFAC Symposium on Fault Detection, Supervision and Safety for Technical Processes*, pp. 268-273, June 2000.

[19] A. Marcos, S. Ganguli and G. Balas, "Application of $\mathcal{H}_\infty$ fault detection and isolation to a Boeing 747-100/200 aircraft", in *AIAA Guidance, Navigation and Control Conference*, Monterey, CA, August 2002.

[20] A. Marcos, D. Mylaraswamy and G. Balas, "Robust Identification and Residual Generation Application to a Turbofan Engine", in *IEEE Aerospace Conference*, vol. 5, pp. 3384-3395, Big Sky, USA, March 2004.

[21] S. Grenaille, D. Henry and A. Zolghadri, "Fault diagnosis in satellites using $\mathcal{H}_\infty$ estimators", in *IEEE International Conference on Systems, Man and Cybernetics*, pp. 5195-5200, 2004

[22] J. Doyle, B. Francis and A. Tannenbaum, *"A feedback control theory"*, MacMillan Publishing, Co., 1990.

[23] K. Zhou and K. Glover, *"Robust and optimal control"*, Prentice-Hall, Englewood Cliffs, NJ, 1996.

[24] G. Balas, J. C. Doyle, K. Glover, A. Packard and R. Smith, "*μ-Analysis and Synthesis Toolbox*", Natick, MA: MUSYN, Inc., and The MathWorks, Inc., 1991.